UNIVERSITI PUTRA MALAYSIA

MECHANICAL, MEDICAL IMAGING AND RADIATION PROPERTIES OF COMPUTED TOMOGRAPHY-BASED KIDNEY PHANTOM EXPLOITING TEXTURAL ANALYSIS

IZDIHAR BINTI KAMAL

FS 2022 39

MECHANICAL, MEDICAL IMAGING AND RADIATION PROPERTIES OF COMPUTED TOMOGRAPHY-BASED KIDNEY PHANTOM EXPLOITING TEXTURAL ANALYSIS

By

IZDIHAR BINTI KAMAL

Thesis Submitted to the School of Graduate Studies, Universiti Putra Malaysia, in Fulfilment of the Requirements for the Degree of Doctor of Philosophy

August 2022

DEDICATION

This work is dedicated to:

The sake of Allah, my Creator, and my Master,

My great teacher and messenger, Nabi Muhammad (May Allah bless and grant him), who taught us the purpose of life,

My great parents, who never stop giving of themselves in countless ways,

My dearest husband, who permitted me to embark this journey,

My dear kids: Amir, Ammar and Afiqah, whom I can't force myself to stop loving.

My dear brothers and sister, who stand by me when things look bleak,

To all my family, the symbol of love and giving,

My friends who encourage and support me,

All the people in my life who touch my heart,

I dedicate this research

Abstract of thesis presented to the Senate of Universiti Putra Malaysia in fulfilment of the requirement for the degree of Doctor of Philosophy

MECHANICAL, MEDICAL IMAGING AND RADIATION PROPERTIES OF COMPUTED TOMOGRAPHY-BASED KIDNEY PHANTOM EXPLOITING TEXTURAL ANALYSIS

By

IZDIHAR BINTI KAMAL

August 2022

Chairman : Muhammad Khalis bin Abdul Karim, PhD
Faculty : Science

Medical imaging phantom has important role in mimicking the properties of human tissue for calibration, training, surgical planning, and simulation purposes. Through standardized quantitative imaging features, the phantom should be able to ascertain information that cannot be visually assessed via radiomic features. Thus, the stability and accuracy of the phantom play significant role in diagnostic imaging especially for the diagnostic performance. This work aimed to introduce an alternative and straightforward polymer-based phantoms with specific mechanical and dielectric properties at the utmost suitable for fabrication of computed tomography-based kidney phantom. To evaluate the influence of Hydrogen Silicone (HS) and water (H_2O) on the compression strength, radiation attenuation properties, and Computed Tomography (CT) number of the blend Polydimethylsiloxane (PDMS) samples as to improve the pure PDMS properties. A polymer blend is a mixture of two and more polymers that have been blended to create a new material with different physical properties. Two phantom based materials; PDMS and silicone elastomer (SE), were investigated for their capabilities to address the requirements. Four samples were prepared with different compositions were studied, and denote as samples S1, S2, S3, and S4, which consisted of PDMS 100%, HS/PDMS 20:80, H_2O/PDMS 20:80, and HS/H_2O/PDMS 20:40:40, respectively. Radiation attenuation properties were evaluated using Phy-X/PSD (Turkey) and XCOM (NIST, USA). The elasticity and dielectric properties of phantom were superior for the blend HS/PDMS 20:80, besides the effective atomic number and linear attenuation coefficient has shown a similar pattern with human kidney tissue at intermediate energy level of 1.50×10^{-2} MeV to 1.5 MeV. PDMS is superior to SE in terms of tensile strength, flexibility, acceptable real part of the complex dielectric constant; $\mathcal{E}_r$ and conductivity which allows it to become a stable kidney phantom for CT scan purposes. Overall, HS/PDMS 20:80 with the use of a 120 kVp X-ray beam, the CT number quantified for sample measured 40 HU and had the highest Contrast-to-Noise Ratio (CNR) value better than pure PDMS. Therefore, the HS/PDMS 20:80 sample formulation exhibited the potential to mimic the human kidney as it has a similar

dynamic and is higher in terms of stability as a medical phantom. In conclusion the blend PDMS as the material of choice to be used as a CT-based kidney phantom in terms of good agreement with compressive strength and radiation attenuation. Notably, the blend PDMS imitates human tissue more precisely and permits a wide range of possibilities for exploiting textural analysis and radiation dosimetry. Hence, it promises to be of value for use in both research and clinical settings for the CT modality as it is physically stable.

Abstrak tesis yang dikemukakan kepada Senat Universiti Putra Malaysia sebagai memenuhi keperluan untuk ijazah Doktor Falsafah

CIRI-CIRI MEKANIKAL, PENGIMEJAN PERUBATAN DAN RADIASI SINARAN BAGI FANTOM BUAH PINGGANG TOMOGRAFI BERKOMPUTER UNTUK ANALISIS TEKSTUR

Oleh

IZDIHAR BINTI KAMAL

Ogos 2022

Pengerusi : Muhammad Khalis bin Abdul Karim, PhD
Fakulti : Sains

Fantom pengimejan perubatan sangat berperanan penting dalam menyerupai sifat tisu manusia untuk tujuan penentukuran, latihan, perancangan pembedahan dan tujuan simulasi. Melalui ciri-ciri pengimejan quantitative, fantom mampu untuk menentukan maklumat yang tidak boleh dilihat menerusi ciri-ciri radiomik. Maka kestabilan dan ketepatan ciri fantom memainkan peranan penting sangat signifikan dalam pengimejan diagnostic untuk menentukan kemampuan diagnostik. Kajian ini bertujuan untuk memperkenalkan fantom berasaskan polimer secara alternatif dan mudah dengan sifat mekanikal dan dielektrik tertentu yang paling sesuai untuk fabrikasi fantom buah pinggang untuk pengimejan tomografi berkomputer. Selain itu, untuk menilai pengaruh Hidrogen Silikon (HS) dan air (H_2O) ke atas kekuatan mampatan, sifat pengecilan sinaran, dan nombor Tomografi Berkomputer (CT) bagi sampel gabungan Polydimethylsiloxane (PDMS) untuk menambah baik sifat PDMS tulen. Gabungan PDMS in terdiri daripada campuran dua atau lebih polimer yang digabung untuk membentuk bahan baru dengan ciri-ciri fizikal yang berbeza. Pertama, dua bahan fantom berasaskan polimer; polydimethylsiloxane (PDMS) dan elastomer silikon (SE), telah dikaji keupayaan mereka untuk memenuhi keperluan. Empat sampel dengan komposisi berbeza telah dikaji, dan mereka termasuk sampel S1, S2, S3, dan S4, yang terdiri daripada PDMS 100%, HS/PDMS 20:80, H_2O/PDMS 20:80, dan HS/H_2O/PDMS 20:40:40, masing-masing. Ciri-ciri pengurangan radiasi dinilai menggunakan simulasi Phy-X/PSD (Turki) dan XCOM (NIST, USA). Keanjalan sampel dan ciri-ciri dielektrik fantom adalah lebih tinggi untuk gabungan HS/PDMS 20:80, disamping itu nombor atom berkesan, pekali pengurangan linear telah menunjukkan corak yang sama dengan tisu buah pinggang manusia pada tahap tenaga pertengahan 1.50 x 10^{-02}MeV hingga 1.5 MeV. PDMS adalah lebih baik daripada SE dari segi kekuatan tegangan, fleksibiliti, bahagian sebenar pemalar dielektrik kompleks yang boleh diterima; $\mathcal{E}_r$ dan kekonduksian yang membolehkannya menjadi fantom buah pinggang yang stabil untuk tujuan pengimejan tomografi berkomputer. Secara keseluruhan , dengan penggunaan pancaran sinar-X 120 kVp, nombor CT yang dikira untuk HS/PDMS 20:80 menunjukkan 40 HU

dan mempunyai nilai Nisbah Kontras-ke-hingar (CNR) tertinggi lebih baik daripada PDMS tulen. Jadi, formulasi sampel HS/PDMS 20:80 mempamerkan potensi untuk menyerupai buah pinggang manusia kerana ia mempunyai dinamik yang sama dan lebih tinggi dari segi kestabilan sebagai fantom perubatan. Kesimpulannya, gabungan PDMS adalah bahan yang dipilih untuk digunakan sebagai fantom tomografi berkomputer kerana berpada nan dengan kekuatan kompresi dan pengurangan radiasi. Terutamanaya gabungan PDMS menyerupai tisu buah pinggang manusia lebih tepat dan membenarkan pelbagai kemungkinan untuk digunakan dalam analisa tekstur dan dosimetri sinaran. Maka, ia menjanjikan nilai untuk digunakan dalam kedua-dua tetapan penyelidikan dan klinikal sebagai alat yang boleh dipercayai untuk pengimejan berkomputer kerana ia adalah stabil secara fizikal.

ACKNOWLEDGEMENTS

Praise and thanks to Allah SWT the Almighty, the Most Gracious, and the Most Merciful for His blessing given to me during my study and in completing this thesis. May Allah's blessing goes to His final Prophet Muhammad (peace be up on him), his family and his companions. First, I would like to express my deepest thanks to my main supervisor, Dr. Muhammad Khalis Karim for the assistance and kind supervision throughout my research journey. I am truly fortunate and grateful to have you as my supervisor, and also to my co-supervisors, Assoc. Prof Dr Syamsiah and Assoc. Prof Dr. Hairil Rashmizal for all the help and knowledge shared throughout my study. I would also like to thank my wonderful family members, especially my parents Hj Kamal and Hajah Fatimah, my husband Abdul Aziz, our children Amir, Ammar, Afiqah and my siblings for always love, understand, and support me throughout this journey. Without their love and support, none of this would have been possible. They had always been there for me, and I am thankful for everything. Not to forget, my lab mate and staffs from Physic department, Faculty of Science for their kind helps and contribution. I would also like to express my thanks to the Dean, Assoc. Prof. Dr Mohd Izham and fellow colleagues especially Aishah and Khairiah in KPJ Healthcare University College for the time and support given. Special thanks also to KPJ Healthcare University College for the financial support throughout my study. Last but not least, to all my fellow students, Nur Zulaika, Wan Nur Syazwani, Nur Athirah, Nur Atiqah Zaaba and Nithiya Ravi Kumar for always make me laugh a little louder, smile a little bigger and live just a little bit better. Thank you again for everyone that involve direct or indirectly throughout my study journey.

This thesis was submitted to the Senate of Universiti Putra Malaysia and has been accepted as fulfilment of the requirement for the degree of Doctor of Philosopy. The members of the Supervisory Committee were as follows:

Muhammad Khalis bin Abdul Karim, PhD
Senior Lecturer
Faculty of Science
Universiti Putra Malaysia
(Chairman)

Hairil Rashmizal bin Abdul Razak, PhD
Associate Professor
Faculty of Medicine and Health Sciences
Universiti Putra Malaysia
(Member)

Syamsiah binti Mashohor, PhD
Associate Professor
Faculty of Engineering
Universiti Putra Malaysia
(Member)

ZALILAH MOHD SHARIFF, PhD
Professor and Dean
School of Graduate Studies
Universiti Putra Malaysia

Date: 10 November 2022

Declaration by graduate student

I hereby confirm that:

- this thesis is my original work;
- quotations, illustrations and citations have been duly referenced;
- this thesis has not been submitted previously or concurrently for any other degree at any institutions;
- intellectual property from the thesis and copyright of thesis are fully-owned by Universiti Putra Malaysia, as according to the Universiti Putra Malaysia (Research) Rules 2012;
- written permission must be obtained from supervisor and the office of Deputy Vice-Chancellor (Research and innovation) before thesis is published (in the form of written, printed or in electronic form) including books, journals, modules, proceedings, popular writings, seminar papers, manuscripts, posters, reports, lecture notes, learning modules or any other materials as stated in the Universiti Putra Malaysia (Research) Rules 2012;
- there is no plagiarism or data falsification/fabrication in the thesis, and scholarly integrity is upheld as according to the Universiti Putra Malaysia (Graduate Studies) Rules 2003 (Revision 2012-2013) and the Universiti Putra Malaysia (Research) Rules 2012. The thesis has undergone plagiarism detection software

Signature: _____ Date: _____

Name and Matric No: Izdihar binti Kamal, _____

Declaration by Members of Supervisory Committee

This is to confirm that:

- the research conducted and the writing of this thesis was under our supervision;
- supervision responsibilities as stated in the Universiti Putra Malaysia (Graduate Studies) Rules 2003 (Revision 2012-2013) are adhered to.

Signature: _____
Name of Chairman of Supervisory Committee: Dr. Muhammad Khalis bin Abdul Karim

Signature: _____
Name of Member of Supervisory Committee: Associate Professor Dr. Hairil Rashmizal bin Abdul Razak

Signature: _____
Name of Member of Supervisory Committee: Dr. Syamsiah Binti Mashohor

TABLE OF CONTENTS

		Page
ABSTRACT		i
ABSTRAK		iii
ACKNOWLEDGEMENTS		v
APPROVAL		vi
DECLARATION		viii
LIST OF TABLES		xiii
LIST OF FIGURES		xv
LIST OF ABBREVIATIONS		xix
CHAPTER		
1	**INTRODUCTION**	1
1.1	Overview	1
1.2	Problem Statement	6
1.3	Research Question	7
1.4	Significant of Study	7
1.5	Research Objective	9
1.5.1	Main Objective	9
1.5.2	Specific Objective	9
1.6	Scope of study	9
1.7	Thesis Outline	10
2	**LITERATURE REVIEW**	11
2.1	Renal cell carcinoma (RCC)	11
2.2	Phantom	12
2.2.1	History of phantom material	12
2.2.2	Computed Tomography Phantom Materials	15
2.2.3	Economical Value of Phantom	17
2.3	Fundamental of polymers	21
2.3.1	Polydimethylsiloxane	21
2.3.2	Silicone Elastomer (SE)	21
2.4	Mechanical behavior of PDMS	22
2.4.1	Compressive behavior of PDMS	24
2.4.2	Dielectric properties	25
2.5	Computed Tomography	29
2.5.1	Imaging properties	30
2.5.2	Signal to Noise Ratio (SNR)	31
2.5.3	Contrast to Noise Ratio (CNR)	32
2.6	Radiation Attenuation Properties	32
2.6.1	Interaction between Photons with Matter	34
2.7	Texture analysis of renal tumor	38
2.7.1	Image Segmentation	38
2.7.2	Feature Extraction	42
2.7.3	First Order Statistics	44
2.7.4	Second-Order Statistical Texture Analysis	46

	2.7.5	Higher-Order Statistical Texture Analysis	50
	2.7.6	Shape Features	51
2.8	Feature Selection		52
2.9	Classification		54
2.10	Summary		54
3	**MATERIALS AND METHOD**		56
3.1	Introduction		56
	3.1.1	Preparation Materials	58
	3.1.2	Fabrication of phantom based PDMS	59
	3.1.3	Fabrication of phantom-based Silicone Elastomer (SE)	60
	3.1.4	Fabrication of Blend PDMS	60
	3.1.5	Polydimethylsiloxane (PDMS) Phantoms with lesion (tumor and stone)	63
	3.1.6	Fabrication of artificial renal stone	63
	3.1.7	Fabrication of kidney tumor phantom	64
	3.1.8	The 3D Printing and Moulding of the Phantoms	66
3.2	Characterization of PDMS, SE and blend PDMS		66
	3.2.1	Density of material	66
	3.2.2	Mechanical test	67
	3.2.3	Dielectric properties	67
	3.2.4	Compression test	69
3.3	Medical Imaging properties: Hounsfield unit (HU) measurement		70
	3.3.1	Computed Tomography	70
	3.3.2	Morphological analysis	70
3.4	Radiation attenuation properties		71
	3.4.1	Software PHY-X/PSD and XCOM	72
3.5	Radiomic analysis study		74
	3.5.1	Data set	74
	3.5.2	Data selection and image acquisition for phantom	75
	3.5.3	3D slicer software for segmentation	75
3.6	Radiomic analysis optimizing features		76
3.7	Feature Selection ANOVA F test		76
3.8	Machine learning tools		79
3.9	Performance Evaluation by using SVM and confusion matrix		80
3.10	Summary		81
4	**RESULT AND DISCUSSION**		82
4.1	Introduction		82
4.2	Structural, Mechanical and Dielectric Properties of PDMS and SE		82
	4.2.1	Physical density of materials	82
	4.2.2	Tensile strength test	83
	4.2.3	Dielectric measurement	86
4.3	Blend Polydimethylsiloxane (PDMS)		89
	4.3.1	Compressive strength of Blend PDMS	89

4.3.2 Medical Imaging Properties of Blend Polydimethylsiloxane Phantoms 91
4.4 Radiation attenuation properties 93
4.4.1 Mass Attenuation Coefficient 93
4.4.2 Half-value layer (HVL) 94
4.4.3 Effective atomic number (Z_{eff}) 94
4.4.4 Exposure buildup factor (EBF) 99
4.4.5 Linear attenuation coefficient 103
4.5 CT number of PDMS samples 103
4.6 Radiomic analysis for Computed Tomography Texture Analysis (CTTA) 108
4.6.1 Comparison between Phantom and RCC Patient 108
4.7 Summary 112
4.8 Limitation and future research 112

5 CONCLUSION AND SUGGESTION 114
5.1 Conclusion 114
5.2 Limitation and Future Research 116

REFERENCES 117
APPENDICES 130
BIODATA OF STUDENT 133
LIST OF PUBLICATIONS 134

LIST OF TABLES

Table		Page
2.1	Fabrication of phantom	19
2.2	Mechanical testing conducted for PDMS and SE	27
2.3	Standard Hounsfield units (HU) of kidney tissue, kidney stone and kidney tumor	30
2.4	Various studies on the radiation attenuation properties	36
2.5	Pros and cons for different segmentation	39
2.6	Implementation of various segmentation techniques	40
2.7	Implementation of Flood -filling algorithm	41
2.8	Description of Texture Analysis	42
2.9	The implementation of texture and shape features in respective fields	44
2.10	The computational formula for histogram-based texture features and explanation	45
2.11	GLCM features and formula	48
2.12	The higher order statistical	50
2.13	Shape feature	52
2.14	ANOVA F-test studies	53
2.15	Implementation of various types of classifiers in previous research	54
3.1	Chemical formulation of PDMS and SE for S1, S2, S3 and S4	58
3.2	Composition of blend PDMS for each sample	61
3.3	Siemens SOMATOM Definition Flash CT scanner	70
3.4	Scanning parameter of the phantom	75
3.5	Features extracted in this research	78
4.1	Density of material	82

4.2	Composition of samples with chemical composition	89
4.3	Average HU number and Image quality of the samples 20 HS:80 PDMS.	92
4.4	Average HU number and Image quality of the samples pure PDMS	92
4.5	Comparison of mass attenuation coefficient (μ/p) estimated by Phy-X/PSD and XCOM	95
4.6	Comparison with the previous studies	98
4.7	Equivalent atomic number (Z_{eq}) and G-P fitting parameters for exposure and EBF and EABF for PDMS S1	100
4.8	Equivalent atomic number (Z_{eq}) and G-P fitting parameters	102
4.9	Comparison of linear attenuation coefficient (cm^{-1}) of each samples and previous works	103
4.10	CT number of each sample is evaluated by quantifying the total photon interaction	104
4.11	The SVM classifier performance	111
5.1	Summary table of properties for phantom and human kidney	114

LIST OF FIGURES

Figure		Page
1.1	Images of the kidney phantom made of different material (a) SE, (b) Agarose gel (c) PDMS	3
1.2	Cross-linking of PDMS	4
1.3	Cross-linking chemistries for silicone elastomer by hydrosilylation reactions	5
1.4	The schematic flow of research framework	8
2.1	Water phantom used for the evaluation of image noise and uniformity. Five ROIs of 25 mm diameter were aligned every 38 mm along the diameter of the phantom	13
2.2	RANDO phantom used in space study [(a) is the front view and (b) is the top view of a slice equipped with thermo-luminescent detectors (TLDs) mounted in polyethylene tubes	13
2.3	The exterior shapes of the MIRD-5 (left) and ORNL-UF (right) phantom models [(a) is the front view and (b) is the side view	14
2.4	Cylindrical mould for tissue mimicking material (TMMs)	15
2.5	Stages involved in the preparation of breast phantom	16
2.6	Visualization of CT and MR images of the phantom	17
2.7	(A) Pelvicalyceal system made from latex gloves. B: Renal parenchymal	18
2.8	Stress strain curve obtained from a tension test	23
2.9	Compression test stress-strain curve	24
2.10	Standard HU numbers scale for human tissues	30
2.11	Region of interest (ROI) delineation in RCC patient, image a) CT scan image of the kidney b) segmented image c) segmentation image in coronal plane d) sagittal plane of the image	42
2.12	Flowchart shows most often encountered radiomics features	43
2.13	Spatial relationships of pixels defined by offsets, where *d* is the distance from the pixel of interest	47

2.14	GLCM computation process	47
2.15	Several feature selections approaches	53
3.1	Methodology of the study	57
3.2	The sample at the top row is SE and at the bottom row is the PDMS samples with different ratios that has been peel out from the petri dish	60
3.3	Step-by-step PDMS and SE fabrication	62
3.4	Blend PDMS with different mixing ratios	63
3.5	Artificial kidney stone	64
3.6	Step-by-step preparation of kidney tumor a) zeroing the weighing scale b) measuring the agarose c) mix the agarose, glycerol and distil water in the beaker d) stir the mixture on the hot plate	65
3.7	Outer mould of the kidney	66
3.8	Schematic illustration of the sample geometry used for tensile testing	67
3.9	(A) Four cured SE samples in a small glass tube. (B) Four cured PDMS samples that has been taken out from the small glass tube	68
3.10	(A) Calibration standard of the probe is set by using a standard sample. (B) PDMS samples are tested to measure the dielectric strength	68
3.11	Cylindrical PDMS for compression test	69
3.12	Compression plate	69
3.13	Example of objective image quality analysis of CT number (mean), image noise (SD), SNR, and CNR by putting the region of interest (ROI) at the middle of sample	71
3.14	Phy-X/PSD software for radiation attenuation measurements	73
3.15	XCOM software	73
3.16	Workflow of radiomic study	74
3.17	Interface of the 3D slicer software, image a) CT scan image of the kidney phantom b) segmented image c) segmentation image in sagittal view for the border of the tumor d) coronal plane of the image	76
3.18	ANOVA f test code set	77

3.19	Flow chart of training model of SVM	80
3.20	Confusion matrix and illustrating the calculation	81
4.1	Stress vs strain for various PDMS mixture	83
4.2	Stress vs strain of Silicone elastomer	84
4.3	Tensile strength for various mixtures and thickness	84
4.4	Elastic modulus for various mixtures and thickness	85
4.5	(a) The real part of the complex dielectric constant Ɛ'r and (b) dielectric loss Ɛ***r***" for various mixtures of PDMS and SE	87
4.6	(Y1) Real part of the complex dielectric constant Ɛ'r of standard PDMS and SE 5/5(Y2) and conductivity s/m (σ) of standard PDMS 10/1 and SE 5/5	88
4.7	Compression Stress–strain plots in (a) 20HS: 80 PDMS, (b) 20 H_20:80PDMS, (c) 20HS:40H_20:40PDMS	89
4.8	Tensile Stress–strain plots in (a) 20HS: 80 PDMS, (b) 20 H_20:80PDMS, (c) 20HS:40H_20:40PDMS	90
4.9	Mass attenuation coefficient (μ/p) as a function of the photon energy and the chemical composition for kidney phantom made from PDMS	97
4.10	Half value layer (HVL) as function of photon energy and chemical composition for kidney phantom made from PDMS	97
4.11	Effective atomic number as function of the photon energy and chemical composition for kidney phantom from various compounds of PDMS	98
4.12	Equivalent atomic number (Z_{eq}) vs. photon energy of each sample	99
4.13	Variations of exposure buildup factor (EBF) on the photon energy for PDMS (a) S0, (b) S1, (c) S2, (d) S3, (e) S4 and (f) S5 samples	106
4.14	Comparison of energy absorption buildup factors (EABF) for various PDMS: (a) 5cm mfp, (b) 15cm mfp, and (c) 40cm mfp	107
4.15	CT scan image of the kidney phantom	108
4.16	AUC- ROC Curve for the SVM model	109
4.17	PRC for the SVM model	110

4.18 The confusion matrix for the tumor VS RCC using the output from the SVM 110

4.19 Depicts the confusion matrix for the kidney VS PDMS using the output from the SVM 111

LIST OF ABBREVIATIONS

ANOVA	Analysis of Variance
CNR	Contrast to Noise Ratio
CT	Computed Tomography
CTTA	CT texture analysis
FN	False Negative
FP	False Positive
AUC	Area under curve
GBD	Global Burden of Disease
GLDM	Gray Level Dependence Matrix
GLRLM	Gray Level Run Length Matrix
GLSZM	Gray Level Size Zone Matrix
HS	Hydrogen silicone
HU	Hounsfield unit
ICRP	International Commission on Radiological Protection
kPa	kilopascal
mGy	milli-gray
ML	Machine Learning
MRI	Magnetic resonance imaging
PDMS	polydimethylsiloxane
PRC	Precision recall curve
RCC	Renal cell carcinoma
RF	Radiomic feature
ROC	Receiver operating characteristic

ROI	Region of Interest
SE	Silicone elastomer
SNR	Signal to Noise Ratio
SVM	Support Vector Machine
TCIA	The Cancer Imaging Archive
TCIA	The Cancer Imaging Archive
TLD	Thermoluminescence dosimeter
TN	True Negative
TP	True Positive
US	ultrasound
UV	Ultraviolet
WHO	World Health Organization

CHAPTER 1

INTRODUCTION

1.1 Overview

Kidney acts as one of the most vital organs in human body. In 2010, 2.3 to 7.1 million people with end-stage kidney disease died without access to dialysis while the Global Burden of Disease (GBD) by World Health Organization (WHO) estimates that 1.2 million people died from kidney failure in 2015. Based on the data from developed countries, renal cell carcinoma (RCC) is considered a malignancy of the 6–7th decade of life and affects younger age (Mittal and Sureka, 2016). Padala et al. (2020) stated that there are 611 cases per 100 000 people with an RCC cumulative risk of 2.8%. This statistic has shown Malaysia to have the highest cumulative risk for RCC incidence among other South-East Asian countries. It is challenging to diagnose the RCC subtype correctly as the interpretation of imaging findings is a subjective process and an accurate prediction the histological RCC subtype strongly depends on the experience and expertise of the radiologist. In addition, due to the lack of validation on a larger scale, the clinical application of these methods is limited (Zhang et al., 2019).

To control the occurrence of renal cancer, early detection of tumor heterogeneity of renal mass is critical. Several imaging techniques for instance ultrasound and analytical methods have been investigated to determine the most accurate and reproducible technique for the differentiation of solid renal masses (Kocak et al., 2018). In recent years ultrasound elastography technics showed increasing development lines, and more studies were performed about elastography on kidneys. The weighted amount of the elastography studies is about chronic kidney disease, kidney failure and allograft patients, while some of them are about kidney masses or diabetic nephropathy (Duymuş et al., 2016). While MRI by using diffusion tensor imaging (DTI) can be used to assess renal dysfunction in chronic kidney diseases. However, because of the significant similarities between malignant and benign renal masses in terms of imaging findings, reliable imaging criteria for the differentiation of these tumors do not exist and remain an essential obstacle before treatment. Under such a condition where human analysis is unfruitful, the unmatched image-processing power of computers in the determination of the characteristics of the lesion has drawn significant interest in the last two decades (Kocak et al., 2018). Despite this alarming data of kidney diseases ranked among the highest to affect people, previous studies on the fabrication of imaging phantoms deliver less exposure to the kidney and its pathologies, compared to other organs such as lungs and liver.

Phantom or so-called artificial organ have discovered their way into a different field of medicine. The use of phantom is a reasonable alternative and may replace with benefit the application of real human tissue. Phantoms can be designed with different sizes, shapes, and compositions to mimic human tissue's properties. The design and composition of a phantom are determined primarily by the purpose of phantom to be

used. Throughout history phantoms have been connected for various reasons. As indicated by their application, they can be sorted as pursues:

i. Imaging phantom is used for calibrating and evaluating of various imaging modalities

ii. Training phantom used for training and testing of interventional procedure

iii. Custom made phantom used for research and development purposes

Imaging phantom used for calibration can be seen in radio photoluminescence (RPL) glass dosimeters used to measure radiation doses set in various organ positions within one year old child anthropomorphic phantom. The organ doses were evaluated from the measurement values and shows that doses for tissues or organs within the scan range were 28–36 mGy in an infant head CT, 3–11 mGy in a chest CT, 5–11 mGy in an abdominal-pelvic CT and 2–14 mGy in a cardiac CT. Hence the differences in the types of CT scanners affects and scan parameters used at each medical facility affect the measurement of the radiation dose. According to Hill et.al iodinated phantom is suitable for use in accurate calibration tools for contrast tomographic imaging in X-ray imaging by showing a promising property of uniformity, stability, and precision of the iodinated material (Hill et. al, 2009)

Phantom was also used as a patient education where a 3D printed model of the renal tumor was used to make the patient understand of their conditions (Bernhard et al., 2016a). The result shows an improvement with the help of their personal 3D kidney model in understanding of basic kidney physiology by 16.7 % ($p = 0.018$), kidney anatomy by 50 % ($p = 0.026$), tumor characteristics by 39.3 % ($p = 0.068$) and the planned surgical procedure by 44.6 % ($p = 0.026$). It was shown that using patient-specific 3D printed phantom is valuable for the patient's understanding. Besides that, Adams et al., (2017) has developed a kidney phantom that would be suitable for surgical simulation, training purpose and development of imaging techniques base on Figure 1.1. According to an author who developed a customized phantom on tissue mimicking material for cardiac tissue phantom to get better precision using a known structure and be used as learning process for imaging operators (Yusof et al., 2017). Medical physicists utilized a phantom to mimic real human tissue that can be used for dosimetry measurement and identification of the limits of a particular system. This phantom could be used to imitate living subjects and prevent unnecessary radiation delivered to human patients.

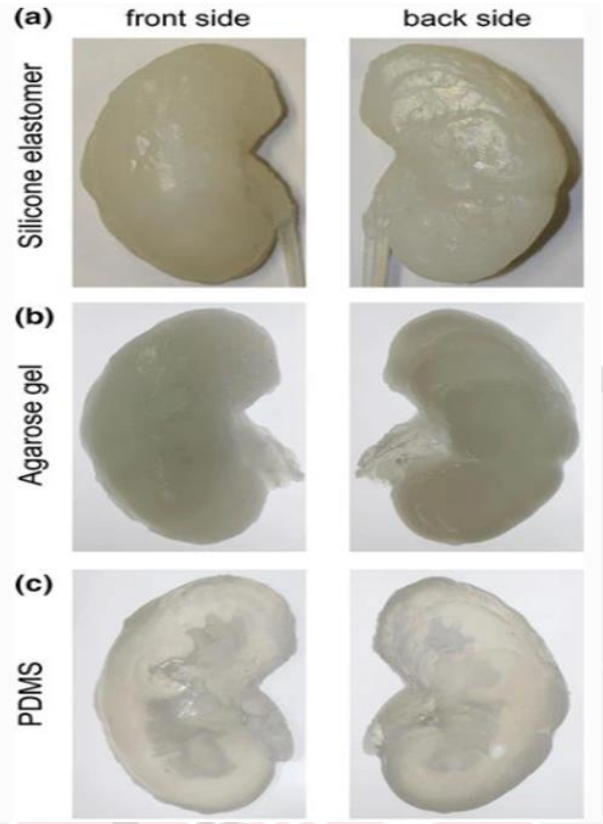

Figure 1.1 : Images of the kidney phantom made of different material (a) SE, (b) Agarose gel (c) PDMS (Adams et al., 2017)

Previously, several materials have been studied and introduced to find the most stable phantom for medical imaging. These materials include agar, silicone, polyvinyl alcohol (PVA), and polyacrylamide (PAA), to mimic human tissues (In, 2016). Agar is easy to prepare but does not have an excellent long-term stability compared to silicone, in which silicone can be considered as a material of choice for a stable phantom. In et al. (2016) has comprehensively reviewed four different types of polymer-based materials for constructing medical phantom: carrageenan-based polymer gel, polymer cross-linked aerogels, UV-curable silicone and self-healing polymer materials (In, 2016). The finding reveals that even though water-based silica and cellulose aerogel phantoms met the imaging properties of human tissues, their volume may shrink, and the fabrication was complex for larger scale production. Nonetheless, a multimodal phantom has been successfully innovated with the use of polydimethylsiloxane (PDMS) and hydrogen silicone (HS) (Hill et.al, 2001; Karimi and Shojaei, 2017). The result demonstrates that the addition of hydrogen silicone could improve mechanical and imaging properties of the phantom. The PDMS or dimethicone, is also a polymer that has been widely used for fabrication and prototyping of microfluidic chips. Briefly, the PDMS empirical formula is $(C_2H_6OSi)n$ and its fragmented formula is $CH_3[Si(CH_3)_2O]nSi(CH3)_3$; where n represents the number of monomers repetitions.

PDMS has an elastic modulus of 360-870 kPa, which is larger than the elastic modulus of a real kidney with 180.32 ± 11.11 kPa (mean $\pm$ SD) and 95.64 ± 9.39 kPa under the axial and transversal loadings, respectively (Karimi and Shojaei, 2017). Elastomers are required to undergo vulcanization process, which is the formation cross-link between long polymer chain. This feature controls the ability of the elastomer to reconfigure its structure when stress is applied, indicating the elasticity. The covalent cross-linkages ensure that the elastomer will return to its original configuration when the stress is removed and would result in a permanent deformation. Cross-links can be introduced into poly-siloxanes by a range of methods, including (i) the use of a tri- or tetra-functional siloxane comonomer during polymerization, (ii) the incorporation of a thermal initiator which will attract hydrogen atoms from PDMS, thus resulting in cross-linking, or (iii) the exposure of PDMS to high energy irradiation. Figure 1.2 shows the method of PDMS cross-linking proposed by previous author (Hill et al., 2001). Cross-linking reactions can also be applied with the intention to improve the surface of cured PDMS sample by using hyperthermal hydrogen induced cross-linking (HHIC)(Bao et al., 2015).

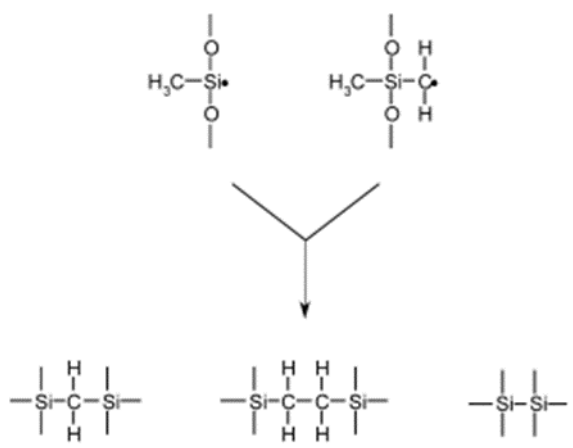

Figure 1.2 : Cross-linking of PDMS (Mazurek et.al 2019)

In this study, the same group of polymers which is known as silicone elastomer (SE) have also been discussed. SE is typically cross-linked using hydrosilylation (usually by Pt-catalysed), condensation (usually by Sn-catalysed) and radical reaction (Mazurek et.al, 2019). In Figure 1.3, the two most used curing chemistries are illustrated. SE is widely used due to its favorable properties, namely flexibility, durable dielectric insulation and its exceptional barrier properties against environmental contaminants. Therefore, it would be beneficial for researchers to compare the effectiveness between PDMS and SE. In this research study, the development of in vitro organ which is kidney was created using a combination of a three-dimensional (3D) printing technique for the outer mould of kidney shape and polymer-based material. Since 3D printing has become the primary method in producing a swiftly prototyping of medical devices and phantom thus allowing for this research to use 3D printing technique as well (Yan et al., 2018). The phantom was created using two material which is silicone elastomer and PDMS with the addition of HS to get the optimum composition that nearest to the human kidney

tissue for comparison (In, 2016). Thus, this research develops and aim to select the best PDMS phantom sample which yields similar mechanical and imaging characteristics to that of real human's kidney tissue and lesions by conducting several assessments to test their properties.

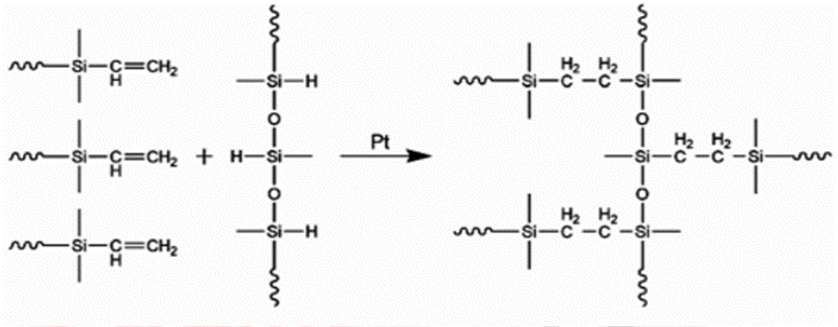

Figure 1.3 : Cross-linking chemistries for silicone elastomer by hydrosilylation reactions (Mazurek et al, 2019)

As the interpretation of imaging findings is a subjective process and a precise prediction on the likelihood of histological renal tumor types strongly depends on the experience and expertise of the radiologist, it is challenging to diagnose the tumor type accurately. This is the conventional way of predicting the heterogeneity of the renal masses. Therefore, opposite characterization of these masses is essential for the clinical management to be instituted precisely.

The radiomics feature of texture analysis intensifies image histogram and can be used as the pipeline after the image processing. The texture analysis of radiomic is an evolving imaging tool to quantify tissue heterogeneity that cannot be perceived by the naked eye (Zhou et al., 2019). Texture analysis is also a promising non-invasive tool for distinguishing renal tumors on CT images (Yu et al., 2017). In this research project, CT texture analysis is used to find the grey level histogram indicating how many pixels of an image share the same grey level. To find the best element in differentiating the types of tumors and quantifying heterogeneity, CT texture analysis image processing would be an innovative technique with various features.

In this study, textural analysis of the radiomic features is used to distinguish the lesion in the kidney phantom which is a tumor, stones and blend PDMS. The tumor in the phantom is compared with the RCC patient, while the blend PDMS is compared to real kidney tissue obtained from CT scan images. These data are the basic information for radiomic feature of the phantom and its difference with RCC will provide a better understanding of the texture analysis. Thus, this can help to reduce the need for biopsy to identify the tumor type present, as the biopsy is a painful procedure. Besides, it increases the accuracy level of prediction of renal masses heterogeneity compared to the quantitative method that uses human ability.

1.2 Problem Statement

The drawback of current designed phantoms faced long-term stability issues due to material insufficiency. Phantoms made of agar and water-based gels demonstrate changes over time due to continuous water expulsion and absorption cycles. This study proposed the potential of stable polymer PDMS is used as phantom kidney material. Fabrication of kidney phantoms with the 3D-printing technique is usually quite costly and difficult to get the exact shape of the phantom due to the printer's limitation.

Additionally, the tissue-equivalency of previously used materials in other studies has not been proved regarding radiation attenuation. Clinically valid anthropomorphic phantoms should demonstrate similar human tissue properties; hence, they should be designed with materials with the same attenuation characteristics. The current PDMS has drawbacks such as a high CT number and low stability, which limits its function as a phantom material like tissue (Miranda et al., 2022). According to In et al. (2016), the modified PDMS with the addition of HS and water is superior to standard PDMS, as the composition reduces its CT number to become relatively close to 40 to 45 HU that closely mimics the kidney tissue (In, 2016).

The photon interaction in various PDMS concentrations for phantom development has not yet been comprehensively discussed. This is also true for pure PDMS. Hence, this study harnesses the theoretical methods in the software to evaluate the mass attenuation coefficient (MAC) compared with other established software based on the computed mixture rule. The polydimethylsiloxane (PDMS) $[(CH3)_2SiO]n$ is by far the most commonly used polymer in siloxane ('silicone') elastomers to imitate physical, optical, and thermal properties (Bernhard et al., 2016b).

In radiomic analysis, the conventional classification systems provide a diagnosis without decision interpretation; where humans cannot directly interpret the results as the systems use low-level features that lack human perception. Several work limits on the potential prognostic and predictive value of texture features on the retrospective image of CT. Figure 1.4 illustrate the schematic framework of the work. In general, the present study is intended to introduce sustainable and economically affordable phantom manufacturing by using commercially available and inexpensive materials. Currently, the PDMS phantom is cost around RM2000 which equivalent to 50 kidney phantoms that has high physical stability and mechanical properties.

CT number from CT images also able to evaluate radiation attenuation criteria specifically for CT scan imaging but not nuclear medicine with different energy levels. Thus, it is worth noting that the effective atomic number (Z_{eff}) and attenuation properties evaluation and help to propose the possibility of the material mimicking the tissue to become an excellent phantom prototype rather than an equivalent value to commensurate the clinical-grade phantom.

1.3 Research Question

i. Which is the best material between polydimethylsiloxane (PDMS) and silicone elastomer (SE) that can optimally mimic human kidney tissue?

ii. What is the advantage of the blend PDMS as the improved formula for the kidney phantom?

iii. What is the radiation attenuation properties of the PDMS and blend PDMS to mimic the human kidney?

iv. Does the radiomic feature of the phantom and kidney show any differences?

1.4 Significant of Study

This research aims to propose modified PDMS as a stable material for fabricating kidney phantom. Several tests on the PDMS samples were performed to ensure their mechanical and medical imaging characteristics matched that of human kidney tissue. Modified PDMS was used instead of its pure form since it is found that the modified material can compensate the limitation of the latter. Different samples with varied mixing ratios were prepared to enable the selection of the best PDMS composition as phantom kidney material.

Manufacturing of polymer-based material for the fabrication of stable kidney phantom led to the introduction of new anthropomorphic phantom which has better stability than previously made water-based phantoms. As the stable phantom allows longer use and functionality with high standard performance.

Several tests were conducted on the phantom samples to ensure that their strength and imaging properties are similar to that of human kidney tissues. The validation of the results can highlight the potential of the sample to act as standard reference phantoms which will allow the evaluation of current and emerging CT techniques. Furthermore, measurement of HU numbers on the lesion particles (kidney stone and tumor) enables us to establish a threshold value for HU numbers of abnormal tissues which will be essential for image characterization.

One promising approach to optimizing radiological assessment is the utilization of radiomics feature analysis which has been shown to perform well for various imaging modalities and classification problems (Yu et al., 2017). Therefore, this study used applied texture analysis to differentiate and classify renal masses to obtain information for better quantifying differences in appearance that the naked eye cannot appreciate.

Overall, this study is significant as it provides information on strength and tissue equivalency of blend PDMS network to be used as a tissue-mimicking kidney phantom.

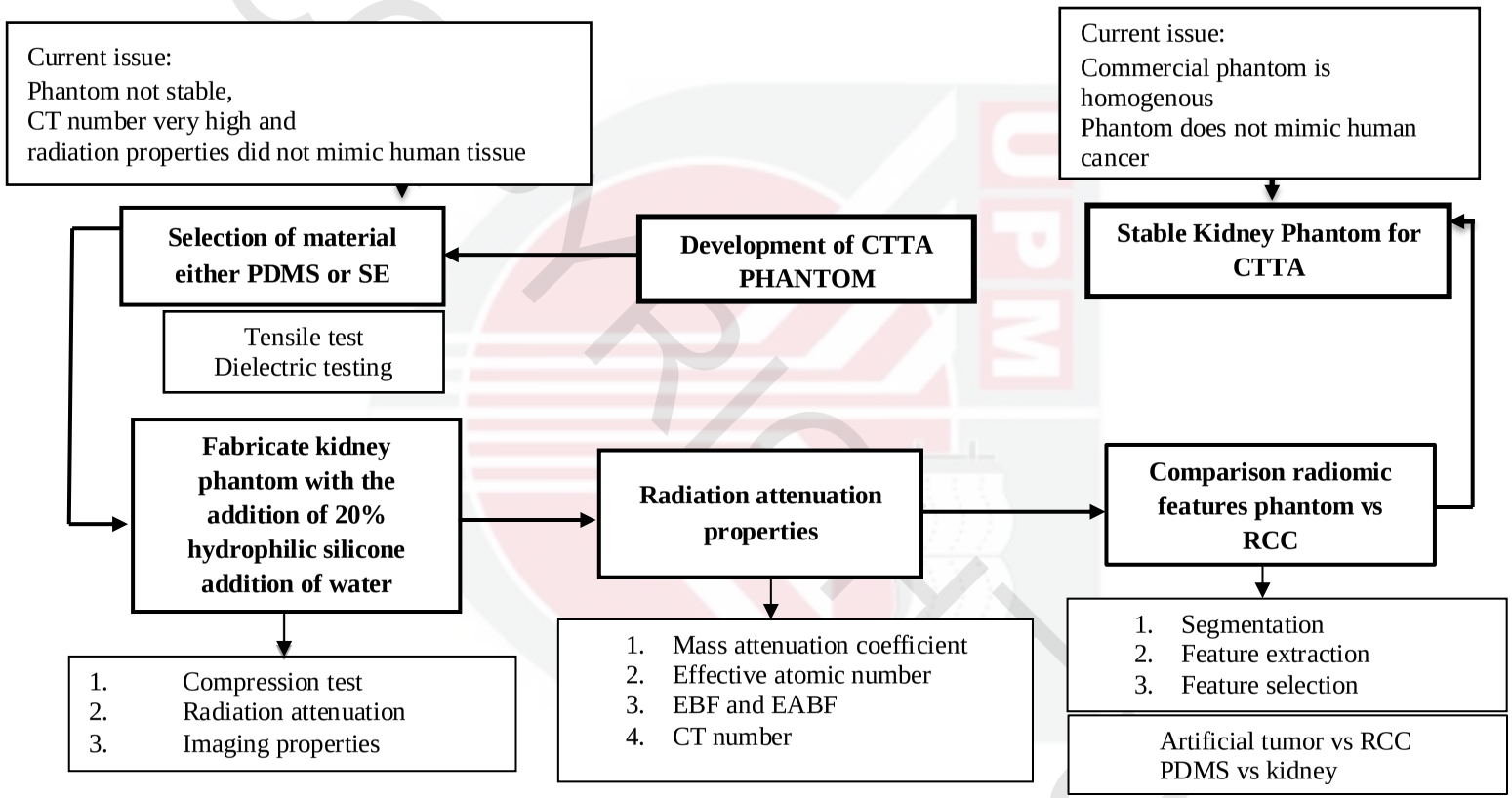

Figure 1.4 : The schematic flow of research framework

1.5 Research Objective

1.5.1 Main Objective

This study aims to develop an alternative method, simple phantoms polymer-based, with specific mechanical, medical imaging and radiation properties to determine whether these are viable phantoms suitable for CTTA. Therefore, this study embarks on the following objective.

1.5.2 Specific Objective

i. To investigate the impact of various formalisms of PDMS and SE on the mechanical and dielectric properties of the fabricated kidney phantom.

ii. To determine the medical imaging property of the blend PDMS for clinical use in CT scan.

iii. To evaluate the radiation properties of the blend PDMS for fabrication of kidney phantom

iv. To evaluate the performance of kidney phantom to RCC patients by using Analysis of Variance (ANOVA) f test with Support Vector Machine (SVM) as a tool for radiomic analysis study.

1.6 Scope of study

The study's scope involves determining the best suit phantom material, characterization, testing and radiomic study. The study was divided into three parts to achieving the objective mentioned beforehand.

i. Part I: Selection of material was made based on PDMS and SE performance as it is more stable than agar based. The size and shape of the phantom was designed based on human kidney and by using 3D printing mould. Besides, the tumor and stone were fabricated to mimic the textured phantom's human tissue.

ii. Part II: Testing and characterizing of material were conducted using tensile test, compression test and dielectrics test according to ASTM polymer standard using Instron 4411 and ASTM D1621 standards using Instron universal compression-testing machine.

iii. Part III: Evaluation of radiation attenuation properties using Phy-X/PSD software and XCOM. Further study on the medical imaging properties by CT scan for the image quality assessment.

iv. Part IV: Radiomic feature extraction by using SVM for the performance evaluation and classifying it with the pathology of the kidney.

1.7 Thesis Outline

This thesis gives a comprehensive overview of the two types of material used to fabricate the kidney phantom: Polydimethylsiloxane (PDMS) and Silicone Elastomer (SE). In Chapter 2, the fundamentals of selected materials, the CT scan process as the scanner of the patient, radiation attenuation theories and radiomic features are briefly explained. In Chapter 3, the materials and methods used are discussed briefly. In Chapter 4, the results and discussion will be presented; the finding of the material mimics the kidney tissue, lesions and radiomic feature finding were explained, respectively. Furthermore, Chapter 5 concludes the results.

REFERENCES

AAPM. (1977). Report n° 3 : Optical radiations in medicine : a survey of uses, measurement and sources. *AAPM Report*, (no 3), 28 p.

Abbasova, N., Yüksel, Z., Abbasov, E., Gülbiçim, H., & Ça, M. (2019). Investigation of gamma-ray attenuation parameters of some materials used in dental applications, *12*(November 2018), 2202–2205. https://doi.org/10.1016/j.rinp.2019.02.068

Abdulsalam, S. O., Mohammed, A. A., Ajao, J. F., Babatunde, R. S., Ogundokun, R. O., Nnodim, C. T., & Arowolo, M. O. (2020). Performance Evaluation of ANOVA and RFE Algorithms for Classifying Microarray Dataset Using SVM. *Lecture Notes in Business Information Processing*, *402*(December), 480–492. https://doi.org/10.1007/978-3-030-63396-7_32

Adams, F., Qiu, T., Mark, A., Fritz, B., Kramer, L., Schlager, D., … Fischer, P. (2017). Soft 3D-Printed Phantom of the Human Kidney with Collecting System. *Annals of Biomedical Engineering*, *45*(4), 963–972. https://doi.org/10.1007/s10439-016-1757-5

Aggarwal, N., & K. Agrawal, R. (2012). First and Second Order Statistics Features for Classification of Magnetic Resonance Brain Images. *Journal of Signal and Information Processing*, *03*(02), 146–153. https://doi.org/10.4236/jsip.2012.32019

Al-Buriahi, M. S., & Tonguc, B. T. (2020). Mass attenuation coefficients, effective atomic numbers and electron densities of some contrast agents for computed tomography. *Radiation Physics and Chemistry*, *166*(August 2019), 108507. https://doi.org/10.1016/j.radphyschem.2019.108507

Alajerami, Y. S. M., Morsy, M. A., Mhareb, M. H. A., Sayyed, M. I., Imheidat, M. A., Hamad, M. K., & Karim, M. K. A. (2021). Structural, optical, and radiation shielding features for a series of borate glassy system modified by molybdenum oxide. *The European Physical Journal Plus*, *136*(5), 583. https://doi.org/10.1140/epjp/s13360-021-01582-x

Alım, Ö. F. Ö. B., & Büyükyıldız, E. Ş. M. (2020). Phy - X / ZeXTRa : a software for robust calculation of effective atomic numbers for photon , electron , proton , alpha particle , and carbon ion interactions. *Radiation and Environmental Biophysics*. https://doi.org/10.1007/s00411-019-00829-7

Arslan, S., Ozyurek, E., & Gunduz-Demir, C. (2014). A color and shape based algorithm for segmentation of white blood cells in peripheral blood and bone marrow images. *Cytometry Part A*, *85*(6), 480–490. https://doi.org/10.1002/cyto.a.22457

Artikboeva, R., Yang, M., Wu, Y., Jie, C., & Heng, Q. (2020). Preparation and Application of the Hydrophilic Amino-Silicone Softener by Emulsion Polymerization. *Advances in Chemical Engineering and Science*, *10*(01), 1–23. https://doi.org/10.4236/aces.2020.101001

Aygün, B. (2020). High alloyed new stainless steel shielding material for gamma and fast neutron radiation. *Nuclear Engineering and Technology*, *52*(3), 647–653. https://doi.org/10.1016/j.net.2019.08.017

Aziz, T., Fan, H., Khan, F. U., Haroon, M., & Cheng, L. (2019). Modified silicone oil types, mechanical properties and applications. *Polymer Bulletin*, *76*(4), 2129–2145. https://doi.org/10.1007/s00289-018-2471-2

Bao, C., Xu, K. Q., Tang, C. Y., Lau, W. M., Yin, C. Bin, Zhu, Y., … Liu, Y. (2015). Cross-linking the surface of cured polydimethylsiloxane via hyperthemal hydrogen projectile bombardment. *ACS Applied Materials and Interfaces*, *7*(16), 8515–8524. https://doi.org/10.1021/acsami.5b00190

Berger, M. J., & Hubbell, J. H. (1987). XCOM : Photon Cross Sections on A National Bureau of Standards.

Bernhard, J. C., Isotani, S., Matsugasumi, T., Duddalwar, V., Hung, A. J., Suer, E., … Gill, I. S. (2016a). Personalized 3D printed model of kidney and tumor anatomy: a useful tool for patient education. *World Journal of Urology*, *34*(3), 337–345. https://doi.org/10.1007/s00345-015-1632-2

Bernhard, J. C., Isotani, S., Matsugasumi, T., Duddalwar, V., Hung, A. J., Suer, E., … Gill, I. S. (2016b). Personalized 3D printed model of kidney and tumor anatomy: a useful tool for patient education. *World Journal of Urology*, *34*(3), 337–345. https://doi.org/10.1007/s00345-015-1632-2

Bock, C., Hospital, F., & Chen, Q. (2009). Thickness-dependent mechanical properties of polydimethylsiloxane membranes, (February). https://doi.org/10.1088/0960-1317/19/3/035028

Böke, A. (2014). Linear attenuation coefficients of tissues from 1 keV to 150 keV. *Radiation Physics and Chemistry*, *102*(9), 1. https://doi.org/https://doi.org/10.1016/j.radphyschem.2014.04.006

Boukhris, I., & Alalawi, A. (2020). Radiation attenuation properties of bioactive glasses doped with NiO. *Ceramics International*, *46*(12), 19880–19889. https://doi.org/10.1016/j.ceramint.2020.05.047

Brynolfsson, P., Nilsson, D., Torheim, T., Asklund, T., Karlsson, C. T., Trygg, J., … Garpebring, A. (2017). Haralick texture features from apparent diffusion coefficient (ADC) MRI images depend on imaging and pre-processing parameters. *Scientific Reports*, *7*(1), 1–11. https://doi.org/10.1038/s41598-017-04151-4

Buch, K., Li, B., Qureshi, M. M., Kuno, H., Anderson, S. W., & Sakai, O. (2017). Quantitative assessment of variation in CT parameters on texture features: Pilot study using a nonanatomic phantom. *American Journal of Neuroradiology*, *38*(5), 981–985. https://doi.org/10.3174/ajnr.A5139

Cannon, L. M., Fagan, A. J., & Browne, J. E. (2011a). Novel tissue mimicking materials for high frequency breast ultrasound phantoms. *Ultrasound in Medicine and Biology*, *37*(1), 122–135. https://doi.org/10.1016/j.ultrasmedbio.2010.10.005

Cannon, L. M., Fagan, A. J., & Browne, J. E. (2011b). Novel tissue mimicking materials for high frequency breast ultrasound phantoms. *Ultrasound in Medicine and Biology*, *37*(1), 122–135. https://doi.org/10.1016/j.ultrasmedbio.2010.10.005

Chiu, T., Xiong, Z., Parsons, D., Folkert, M. R., Medin, P. M., & Hrycushko, B. (2020). Low-cost 3D print–based phantom fabrication to facilitate interstitial prostate brachytherapy training program. *Brachytherapy*, *19*(6), 800–811. https://doi.org/10.1016/j.brachy.2020.06.015

Chmarra, M. K., Hansen, R., Mårvik, R., & Langø, T. (2013). Multimodal Phantom of Liver Tissue. *PLoS ONE*, *8*(5), 1–9. https://doi.org/10.1371/journal.pone.0064180

Chu, P. M., Cho, S., Huang, K., & Cho, K. (2019). Flood-fill-based object segmentation and tracking for intelligent vehicles. *International Journal of Advanced Robotic Systems*, *16*(6), 1–11. https://doi.org/10.1177/1729881419885206

Chu, P. M., Cho, S., Park, Y. W., & Cho, K. (2017). Fast point cloud segmentation based on flood-fill algorithm. *IEEE International Conference on Multisensor Fusion and Integration for Intelligent Systems*, *2017-Novem*(Mfi), 656–659. https://doi.org/10.1109/MFI.2017.8170397

Ciecholewski, M. (2017). Malignant and benign mass segmentation in mammograms using active contour methods. *Symmetry*, *9*(11). https://doi.org/10.3390/sym9110277

Crook, M. N. (1937). Visual discrimination of movement. *Journal of Psychology: Interdisciplinary and Applied*, *3*(2), 541–558. https://doi.org/10.1080/00223980.1937.9917520

Dewerd, L. A., & Kissick, M. (2014). *Biological and Medical Physics, Biomedical Engineering The Phantoms of Medical and Health Physics: Devices for Research and Development*. Retrieved from http://www.springer.com/series/3740

Dey, S. K., & Mahbubur, R. M. (2019). Effects of Machine Learning Approach in Flow-Based. *Symmetry*, *12*(7), 1–21.

Ding, C., & Peng, H. (2003). Minimum redundancy feature selection from microarray gene expression data. *Proceedings of the 2003 IEEE Bioinformatics Conference, CSB 2003*, *3*(2), 523–528. https://doi.org/10.1109/CSB.2003.1227396

Duymuş, M., Menzilcioğlu, M. S., Gök, M., & Avcu, S. (2016). Kidney Ultrasound Elastography: Review. *Kafkas Journal of Medical Sciences*, *6*(2), 121–129. https://doi.org/10.5505/kjms.2016.60490

Elssied, N. O. F., Ibrahim, O., & Osman, A. H. (2014). A novel feature selection based on one-way ANOVA F-test for e-mail spam classification. *Research Journal of Applied Sciences, Engineering and Technology*, *7*(3), 625–638. https://doi.org/10.19026/rjaset.7.299

Gabriel, C., Gabriel, S., & Corthout, E. (1996). The dielectric properties of biological tissues: I. Literature survey. *Physics in Medicine and Biology*, *41*(11), 2231–2249. https://doi.org/10.1088/0031-9155/41/11/001

Galloway, M. M. (1975). Texture analysis using gray level run lengths. *Computer Graphics and Image Processing*, *4*(2), 172–179. https://doi.org/10.1016/s0146-664x(75)80008-6

Ganeshan, B., Khalvati, F., Kiss, A., Vosough, A., Bjarnason, G. A., & Haider, M. A. (2017). CT texture analysis: a potential tool for prediction of survival in patients with metastatic clear cell carcinoma treated with sunitinib. *Cancer Imaging*, *17*(1), 1–9. https://doi.org/10.1186/s40644-017-0106-8

Gaudière, F., Masson, I., Morin-Grognet, S., Thoumire, O., Vannier, J. P., Atmani, H., … Labat, B. (2012). Mechano-chemical control of cell behaviour by elastomer templates coated with biomimetic Layer-by-Layer nanofilms. *Soft Matter*, *8*(32), 8327–8337. https://doi.org/10.1039/c2sm25614b

Gerward, L., Guilbert, N., Jensen, K. B., & Levring, H. (2004). WinXCom — a program for calculating X-ray attenuation coefficients, *71*, 653–654. https://doi.org/10.1016/j.radphyschem.2004.04.040

Grantham, K., Li, H., Zhao, T., & Klein, E. (2014). SU-E-CAMPUS-J-06: The Impact of CT-Scan Energy On Range Uncertainty in Proton Therapy Planning. *Medical Physics*, *41*(6Part22), 387–387. https://doi.org/10.1118/1.4889026

Greening, G. J., Istfan, R., Higgins, L. M., Balachandran, K., Roblyer, D., Pierce, M. C., & Muldoon, T. J. (2014). Characterization of thin poly(dimethylsiloxane)-based tissue-simulating phantoms with tunable reduced scattering and absorption coefficients at visible and near-infrared wavelengths. *Journal of Biomedical Optics*, *19*(11), 115002. https://doi.org/10.1117/1.jbo.19.11.115002

Greffier, J., Macri, F., Larbi, A., Fernandez, A., Pereira, F., Mekkaoui, C., & Beregi, J. P. (2016). Dose reduction with iterative reconstruction in multi-detector CT: What is the impact on deformation of circular structures in phantom study? *Diagnostic and Interventional Imaging*, *97*(2), 187–196. https://doi.org/10.1016/j.diii.2015.06.019

Haj-Hosseini, N., Kistler, B., & Wårdell, K. (2014). Development and characterization of a brain tumor mimicking fluorescence phantom. *Design and Performance Validation of Phantoms Used in Conjunction with Optical Measurement of Tissue VI*, *8945*, 894505. https://doi.org/10.1117/12.2039861

Halgunset, J., Rethy, A., Hofstad, E. F., Sæternes, J. O., Mårvik, R., Sánchez-Margallo, J. A., & Langø, T. (2017). Anthropomorphic liver phantom with flow for multimodal image-guided liver therapy research and training. *International Journal of Computer Assisted Radiology and Surgery*, *13*(1), 61–72. https://doi.org/10.1007/s11548-017-1669-3

Haniff, N. S. M., Karim, M. K. A., Osman, N. H., Saripan, M. I., Isa, I. N. C., & Ibahim, M. J. (2021). Stability and reproducibility of radiomic features based various segmentation technique on mr images of hepatocellular carcinoma (Hcc). *Diagnostics*, *11*(9). https://doi.org/10.3390/diagnostics11091573

Harun, H. H., Abdul Karim, M. K., Abd Rahman, M. A., Abdul Razak, H. R., Che Isa, I. N., & Harun, F. (2020). Establishment of CTPA Local Diagnostic Reference Levels with Noise Magnitude as a Quality Indicator in a Tertiary Care Hospital. *Diagnostics*, *10*(9), 1–11. https://doi.org/10.3390/diagnostics10090680

Heimann, P. . (1968). Moseley's Interpretation of X-Ray Spectra, *12*(4), 261–274.

Hill, D. J. T., Preston, C. M. L., Salisbury, D. J., & Whittaker, A. K. (2001). Molecular weight changes and scission and crosslinking in poly(dimethyl siloxane) on gamma radiolysis. *Radiation Physics and Chemistry*, *62*(1), 11–17. https://doi.org/10.1016/S0969-806X(01)00416-9

Hill, M. L., Mainprize, J. G., Mawdsley, G. E., & Yaffe, M. J. (2009). A solid iodinated phantom material for use in tomographic x-ray imaging. *Medical Physics*, *36*(10), 4409–4420. https://doi.org/10.1118/1.3213516

Htay, T. T., & Maung, S. S. (2018). Early Stage Breast Cancer Detection System using GLCM feature extraction and K-Nearest Neighbor (k-NN) on Mammography image. *ISCIT 2018 - 18th International Symposium on Communication and Information Technology*, (Iscit), 345–348. https://doi.org/10.1109/ISCIT.2018.8587920

Hubbell, J. H. (1982). Photon mass attenuation and energy-absorption coefficients. *The International Journal Of Applied Radiation And Isotopes*, *33*(11), 1269–1290. https://doi.org/10.1016/0020-708X(82)90248-4

Hwang, J., Kim, H.-J., Lemaillet, P., Wabnitz, H., Grosenick, D., Yang, L., … Pogue, B. (2017). Polydimethylsiloxane tissue-mimicking phantoms for quantitative optical medical imaging standards. In R. Raghavachari, R. Liang, & T. J. Pfefer (Eds.), *Design and Quality for Biomedical Technologies X* (Vol. 10056, p. 1005603). https://doi.org/10.1117/12.2263379

I D Johnston, D K McCluskey, C. K. L. T. and M. C. T. (2014). Mechanical characterization of bulk Sylgard 184 for microfluidics and microengineering Related content. *Journal of Micromechanics and Microengineering*, *24 (2014)*(035017), 7pp. https://doi.org/10.1088/0960-1317/24/3/035017

In, E. (2016). Development of Polymer-based Gels for Multimodal Medical Imaging Phantoms, 122.

Inglis, S., Ramnarine, K. V., Plevris, J. N., & McDicken, W. N. (2006). An anthropomorphic tissue-mimicking phantom of the oesophagus for endoscopic ultrasound. *Ultrasound in Medicine and Biology*, *32*(2), 249–259. https://doi.org/10.1016/j.ultrasmedbio.2005.10.005

Issa, S. A., Zakaly, H. M. H., Pyshkina, M., Mostafa, M. Y. A., Rashad, M., & Soliman, T. S. (2021). Structure, optical, and radiation shielding properties of PVA–BaTiO3 nanocomposite films: An experimental investigation. *Radiation Physics and Chemistry*, *180*, 109281. https://doi.org/10.1016/j.radphyschem.2020.109281

Jaime, R. A. O., Basto, R. L. Q., Lamien, B., Orlande, H. R. B., Eibner, S., & Fudym, O. (2013). Fabrication methods of phantoms simulating optical and thermal properties. *Procedia Engineering*, *59*, 30–36. https://doi.org/10.1016/j.proeng.2013.05.090

Jang, H., Joshua Pfefer, T., & Chen, Y. (2015). Solid hemoglobin-polymer phantoms for evaluation of biophotonic systems. *Optics Letters*, *40*(18), 4321. https://doi.org/10.1364/ol.40.004321

Jung, H. (2021). Basic Physical Principles and Clinical Applications of Computed Tomography. *Progress in Medical Physics*, *32*(1), 1–17. https://doi.org/10.14316/pmp.2021.32.1.1

Karim, M. K. A., Rahim, N. A., Matsubara, K., Hashim, S., Mhareb, M. H. A., & Musa, Y. (2019). The effectiveness of bismuth breast shielding with protocol optimization in CT Thorax examination. *Journal of X-Ray Science and Technology*, *27*(1), 139–147. https://doi.org/10.3233/XST-180397

Karimi, A., & Shojaei, A. (2017). Measurement of the Mechanical Properties of the Human Kidney. *Irbm*, *38*(5), 292–297. https://doi.org/10.1016/j.irbm.2017.08.001

Kaufman, J. G., & Rooy, E. L. (2021). Stress-Strain Curves. *Aluminum Alloy Castings*, 193–209. https://doi.org/10.31399/asm.tb.aacppa.t51140193

Kazanowski, P., Aluminum, H., Tubing, P., Dickson, R., & Aluminum, H. (2015). Evaluation of Process Mechanism and Parameters for Automated Stretching Line, (May 2012), 327–342.

Khlystov, N., & Zheng, J. (2013). Uniaxial Tension and Compression Testing of Materials, 1–19.

Kim, T. Y., Cho, N. H., Jeong, G. B., Bengtsson, E., & Choi, H. K. (2014). 3D texture analysis in renal cell carcinoma tissue image grading. *Computational and Mathematical Methods in Medicine*, *2014*. https://doi.org/10.1155/2014/536217

King, B. W., Landheer, K. A., & Johns, P. C. (2011). X-ray coherent scattering form factors of tissues, water and plastics using energy dispersion. *Physics in Medicine and Biology*, *56*(14), 4377–4397. https://doi.org/10.1088/0031-9155/56/14/010

Kirby, B. J., Davis, J. R., Grand, J. A., & Morgan, M. J. (2003). Extracting material parameters from x-ray attenuation: A CT feasibility study using kilovoltage synchrotron x-rays incident upon low atomic number absorbers. *Physics in Medicine and Biology*. https://doi.org/10.1088/0031-9155/48/20/009

Kocak, B., Ates, E., Durmaz, E. S., Ulusan, M. B., & Kilickesmez, O. (2019). Influence of segmentation margin on machine learning–based high-dimensional quantitative CT texture analysis: a reproducibility study on renal clear cell carcinomas. *European Radiology*. https://doi.org/10.1007/s00330-019-6003-8

Kocak, B., Yardimci, A. H., Bektas, C. T., Turkcanoglu, M. H., Erdim, C., Yucetas, U., … Kilickesmez, O. (2018). Textural differences between renal cell carcinoma subtypes: Machine learning-based quantitative computed tomography texture analysis with independent external validation. *European Journal of Radiology*, *107*, 149–157. https://doi.org/10.1016/j.ejrad.2018.08.014

Kumar, B. J., Naveen, H., Kumar, B. P., Sharma, S. S., & Villegas, J. (2018). Logistic regression for polymorphic malware detection using ANOVA F-Test. *Proceedings of 2017 International Conference on Innovations in Information, Embedded and Communication Systems, ICIIECS 2017*, *2018-Janua*, 1–5. https://doi.org/10.1109/ICIIECS.2017.8275880

Kurudirek, M. (2014). Effective atomic numbers , water and tissue equivalence properties of human tissues , tissue equivalents and dosimetric materials for total electron interaction in the energy region 10 keV – 1 GeV. *Applied Radiation and Isotopes*, *94*, 1–7. https://doi.org/10.1016/j.apradiso.2014.07.002

Lan, T., Naguib, H. E., & Coolens, C. (2017). Development of a permeable phantom for dynamic contrast enhanced (DCE) imaging quality assurance: material characterization and testing. *Biomedical Physics & Engineering Express*, *3*(2), 025018. https://doi.org/10.1088/2057-1976/aa6486

Li, W., Belmont, B., Greve, J. M., Manders, A. B., Downey, B. C., Zhang, X., … Shih, A. (2016). Polyvinyl chloride as a multimodal tissue-mimicking material with tuned mechanical and medical imaging properties. *Medical Physics*, *43*(10), 5577–5592. https://doi.org/10.1118/1.4962649

Li, Z., Zhou, Z., Li, Y., & Tang, S. (n.d.). Effect of Cyclic Loading on Surface Instability of Silicone Rubber under Compression. *Polymers 2017, 9(4), 148*, 1–13. https://doi.org/10.3390/polym9040148

Liakhov, E., Smolyanskaya, O., Popov, A., Odlyanitskiy, E., Balbekin, N., & Khodzitsky, M. (2016). Fabrication and characterization of biotissue-mimicking phantoms in the THz frequency range. *Journal of Physics: Conference Series*, *735*(1). https://doi.org/10.1088/1742-6596/735/1/012080

Liu, M., Sun, J., Sun, Y., Bock, C., & Chen, Q. (2009). Thickness-dependent mechanical properties of polydimethylsiloxane membranes. *Journal of Micromechanics and Microengineering*, *19*(3). https://doi.org/10.1088/0960-1317/19/3/035028

Liu, Z., Wang, S., Dong, D., Wei, J., Fang, C., Zhou, X., … Tian, J. (2019). The applications of radiomics in precision diagnosis and treatment of oncology: Opportunities and challenges. *Theranostics*, *9*(5), 1303–1322. https://doi.org/10.7150/thno.30309

MacKin, D., Ger, R., Dodge, C., Fave, X., Chi, P. C., Zhang, L., … Court, L. (2018). Effect of tube current on computed tomography radiomic features. *Scientific Reports*, *8*(1), 1–10. https://doi.org/10.1038/s41598-018-20713-6

Mall, P. K., Singh, P. K., & Yadav, D. (2019). GLCM based feature extraction and medical X-RAY image classification using machine learning techniques. *2019 IEEE Conference on Information and Communication Technology, CICT 2019*, (December). https://doi.org/10.1109/CICT48419.2019.9066263

Manickam, K., Reddy, M. R., Seshadri, S., & Raghavan, B. (2015). Development of a training phantom for compression breast elastography—comparison of various elastography systems and numerical simulations. *Journal of Medical Imaging*, *2*(4), 047002. https://doi.org/10.1117/1.jmi.2.4.047002

Manjunatha, H. C. (2015). Comparison of effective atomic numbers of the cancerous and normal kidney tissue (pp. 83–91). https://doi.org/10.4103/0972-0464.169376

Manohara, S. R., Hanagodimath, S. M., & Gerward, L. (2011). Energy absorption buildup factors of human organs and tissues at energies and penetration depths relevant for radiotherapy and diagnostics, *12*(4), 296–312.

Mata, A., & Fleischman, A. J. (2005). Characterization of Polydimethylsiloxane (PDMS) Properties for Biomedical Micro / Nanosystems, *2*, 281–293.

Mazurek, P. (2019). Chem Soc Rev How to tailor flexible silicone elastomers with mechanical integrity : a tutorial review, 1448–1464. https://doi.org/10.1039/c8cs00963e

Mazurek, P., Vudayagiri, S., & Skov, A. L. (2019). How to tailor flexible silicone elastomers with mechanical integrity: A tutorial review. *Chemical Society Reviews*, *48*(6), 1448–1464. https://doi.org/10.1039/c8cs00963e

Michiels, S., D'Hollander, A., Lammens, N., Kersemans, M., Zhang, G., Denis, J. M., … Depuydt, T. (2016). Towards 3D printed multifunctional immobilization for proton therapy: Initial materials characterization. *Medical Physics*, *43*(10), 5392–5402. https://doi.org/10.1118/1.4962033

Miranda, I., Souza, A., Sousa, P., Ribeiro, J., Castanheira, E. M. S., Lima, R., & Minas, G. (2022). Properties and applications of PDMS for biomedical engineering: A review. *Journal of Functional Biomaterials*, *13*(1). https://doi.org/10.3390/jfb13010002

Mittal, M. K., & Sureka, B. (2016). Solid renal masses in adults. *Indian Journal of Radiology and Imaging*, *26*(4), 429–442. https://doi.org/10.4103/0971-3026.195773

Mohanty, A. K., Beberta, S., & Lenka, S. K. (2011). Classifying Benign and Malignant Mass using GLCM and GLRLM based Texture Features from Mammogram. *International Journal of Engineering Research and Applications (IJERA)*, *1*(3), 687–693.

Mohd Yusof, N. S., Dewi, D. E. O., Mohd Faudzi, A. 'Athif, Md Salih, N., Abu Bakar, N., & Abdul Hamid, H. (2017). Ultrasound imaging characterization on tissue mimicking materials for cardiac tissue phantom: Texture analysis perspective. *Malaysian Journal of Fundamental and Applied Sciences*, *13*(4–2), 501–508. https://doi.org/10.11113/mjfas.v13n4-2.822

Mori, S., Endo, M., Nishizawa, K., Ohno, M., Miyazaki, H., Tsujita, K., & Saito, Y. (2005). Prototype heel effect compensation filter for cone-beam CT. *Physics in Medicine and Biology*, *50*(22), 359–370. https://doi.org/10.1088/0031-9155/50/22/N02

Muhammad, N. A., Kayun, Z., Abu Hassan, H., Wong, J. H. D., Ng, K. H., & Karim, M. K. A. (2021). Evaluation of Organ Dose and Image Quality Metrics of Pediatric CT Chest-Abdomen-Pelvis (CAP) Examination: An Anthropomorphic Phantom Study. *Applied Sciences*, *11*(5), 2047. https://doi.org/10.3390/app11052047

Mull, R. T. (1984). Mass estimates by computed tomography: Physical density from CT numbers. *American Journal of Roentgenology*, *143*(5), 1101–1104. https://doi.org/10.2214/ajr.143.5.1101

Nayak, T., Bhat, N., Bhat, V., Shetty, S., Javed, M., & Nagabhushan, P. (2019). *Automatic segmentation and breast density estimation for cancer detection using an efficient watershed algorithm. Lecture Notes in Networks and Systems* (Vol. 43). Springer Singapore. https://doi.org/10.1007/978-981-13-2514-4_29

Nemavhola, F., & Sigwadi, R. (2019). Prediction of hyperelastic material properties of Nafion117 and Nafion/ZrO2 nano-composite membrane. *International Journal of Automotive and Mechanical Engineering*, *16*(2), 6524–6540. https://doi.org/10.15282/ijame.16.2.2019.5.0492

Nikoo, H., Talebi, H., & Mirzaei, A. (2011). A supervised method for determining displacement of Gray Level Co-occurrence Matrix. *2011 7th Iranian Conference on Machine Vision and Image Processing, MVIP 2011 - Proceedings*, 1–5. https://doi.org/10.1109/IranianMVIP.2011.6121563

Oh, Y., Park, S., & Ye, J. C. (2020). Deep Learning COVID-19 Features on CXR Using Limited Training Data Sets. *IEEE Transactions on Medical Imaging*, *39*(8), 2688–2700. https://doi.org/10.1109/TMI.2020.2993291

Omar, N., Mohamad, M. M., & Paimin, A. N. (2015). Dimension of Learning Styles and Students' Academic Achievement. *Procedia - Social and Behavioral Sciences*, *204*, 172–182. https://doi.org/10.1016/j.sbspro.2015.08.130

Opik, R., Hunt, A., Ristolainen, A., Aubin, P. M., & Kruusmaa, M. (2012a). Development of high fidelity liver and kidney phantom organs for use with robotic surgical systems. *Proceedings of the IEEE RAS and EMBS International Conference on Biomedical Robotics and Biomechatronics*, (June), 425–430. https://doi.org/10.1109/BioRob.2012.6290831

Opik, R., Hunt, A., Ristolainen, A., Aubin, P. M., & Kruusmaa, M. (2012b). Development of high fidelity liver and kidney phantom organs for use with robotic surgical systems. *Proceedings of the IEEE RAS and EMBS International Conference on Biomedical Robotics and Biomechatronics*, 425–430. https://doi.org/10.1109/BioRob.2012.6290831

Öztürk, Ş., & Akdemir, B. (2018). Application of Feature Extraction and Classification Methods for Histopathological Image using GLCM, LBP, LBGLCM, GLRLM and SFTA. *Procedia Computer Science*, *132*(Iccids), 40–46. https://doi.org/10.1016/j.procs.2018.05.057

Padala, S. A., Barsouk, A., Thandra, K. C., Saginala, K., Mohammed, A., Vakiti, A., … Barsouk, A. (2020). Epidemiology of renal cell carcinoma. *World Journal of Oncology*, *11*(3), 79–87. https://doi.org/10.14740/WJON1279

Padhi, S., Rup, S., Saxena, S., & Mohanty, F. (2019). Mammogram segmentation methods: A brief review. *2019 2nd International Conference on Intelligent Communication and Computational Techniques, ICCT 2019*, (June 2021), 218–223. https://doi.org/10.1109/ICCT46177.2019.8968781

Pan, Y., Zhu, F., Fan, J., Tao, J., Lin, X., Wang, F., & Shi, L. (2018). Investigation of mechanical properties of silicone/phosphor composite used in light emitting diodes package. *Polymers*, *10*(2). https://doi.org/10.3390/polym10020195

Peper, J. S., & Dahl, R. E. (2016). Radiomics: a new application from established techniques. *Expert Review of Precision Medicine and Drug Development*, *1*(2), 207–226. https://doi.org/10.1080/23808993.2016.1164013.Radiomics

Ramola, A., Shakya, A. K., & Van Pham, D. (2020). Study of statistical methods for texture analysis and their modern evolutions. *Engineering Reports*, *2*(4), 1–24. https://doi.org/10.1002/eng2.12149

Rasyid, M. B. Al, Yunidar, Arnia, F., & Munadi, K. (2018). Histogram statistics and GLCM features of breast thermograms for early cancer detection. *1st International ECTI Northern Section Conference on Electrical, Electronics, Computer and Telecommunications Engineering, ECTI-NCON 2018*, 120–124. https://doi.org/10.1109/ECTI-NCON.2018.8378294

Reddy, V. N., & Rao, P. S. (2018). Comparative analysis of breast cancer detection using K-means and FCM & EM segmentation techniques. *Ingenierie Des Systemes d'Information*, *23*(6), 173–187. https://doi.org/10.3166/ISI.23.6.173-187

Şakar, E., Özpolat, Ö. F., Alım, B., Sayyed, M. I., & Kurudirek, M. (2020). Phy-X / PSD: Development of a user friendly online software for calculation of parameters relevant to radiation shielding and dosimetry. *Radiation Physics and Chemistry*, *166*(August 2019). https://doi.org/10.1016/j.radphyschem.2019.108496

Sardar, V. B., Rajhans, N. R., Pathak, A., & Prabhu, T. (2016). Development in Silicone Material for Biomedical Applications 14 th International Conference on Humanizing Work and Work Environment HWWE-2016 Developments in silicone material for biomedical applications- A review, (December).

Seethapathy, S., & Górecki, T. (2012). Applications of polydimethylsiloxane in analytical chemistry: A review. *Analytica Chimica Acta*, *750*, 48–62. https://doi.org/10.1016/j.aca.2012.05.004

Septian, R., & Adi, K. (2020). Validation of Affordable and Applicable Kidney Phantom Model (Aarm) for Ultrasound-Guided Percutaneous Nephrostomy Simulation. *Indonesian Journal of Urology*, *27*(1), 26–33. https://doi.org/10.32421/juri.v27i1.515

Shan, J., Alam, S. K., Garra, B., Zhang, Y., & Ahmed, T. (2016). Computer-Aided Diagnosis for Breast Ultrasound Using Computerized BI-RADS Features and Machine Learning Methods. *Ultrasound in Medicine and Biology*, *42*(4), 980–988. https://doi.org/10.1016/j.ultrasmedbio.2015.11.016

Singam, P., Ho, C., Hong, G. E., Mohd, A., Tamil, A. M., Cheok, L. B., & Zainuddin, Z. (2010). Clinical characteristics of renal cancer in Malaysia: A ten year review. *Asian Pacific Journal of Cancer Prevention*, *11*(2), 503–506.

Sombatsompop, N., & Chaochanchaikul, K. (2004). Effect of moisture content on mechanical properties, thermal and structural stability and extrudate texture of poly(vinyl chloride)/wood sawdust composites. *Polymer International*, *53*(9), 1210–1218. https://doi.org/10.1002/pi.1535

Souza, J. C., Silva, T. F. B., Rocha, S. V., Paiva, A. C., Braz, G., Almeida, J. D. S., & Silva, A. C. (2018). Classification of Malignant and Benign Tissues in Mammography using Dental Shape Descriptors and Shape Distribution, 5 (6 .)-5 (6 .). https://doi.org/10.1049/ic.2017.0030

Umale, S., Deck, C., Bourdet, N., Dhumane, P., Soler, L., Marescaux, J., & Willinger, R. (2013). Experimental mechanical characterization of abdominal organs: Liver, kidney & spleen. *Journal of the Mechanical Behavior of Biomedical Materials*, *17*, 22–33. https://doi.org/10.1016/j.jmbbm.2012.07.010

Varghese, B. A., Hwang, D., Cen, S. Y., Levy, J., Liu, D., Lau, C., … Duddalwar, V. A. (2019). Reliability of CT-based texture features: Phantom study. *Journal of Applied Clinical Medical Physics*, *20*(8), 155–163. https://doi.org/10.1002/acm2.12666

Vos, N., & Oyen, R. (2018). Renal angiomyolipoma: The good, the bad, and the ugly. *Journal of the Belgian Society of Radiology*, *102*(1), 1–9. https://doi.org/10.5334/jbsr.1536

Wang, Z. (2011). Polydimethylsiloxane Mechanical Properties Measured by Macroscopic Compression and Nanoindentation Techniques.

Wang, Z., Volinsky, A. A., & Gallant, N. D. (2014). Crosslinking Effect on Polydimethylsiloxane Elastic Modulus Measured by Custom-Built Compression Instrument, *41050*, 1–4. https://doi.org/10.1002/app.41050

Wróbel, M. S., Popov, A. P., Bykov, A. V., Tuchin, V. V., & Jędrzejewska-Szczerska, M. (2016). Nanoparticle-free tissue-mimicking phantoms with intrinsic scattering. *Biomedical Optics Express*, *7*(6), 2088. https://doi.org/10.1364/boe.7.002088

Wu, H., Chiu, D. T., Anderson, J. R., Duffy, D. C., Whitesides, G. M., McDonald, J. C., & Schueller, O. J. (2000). Fabrication of microfluidic systems in poly(dimethylsiloxane). *Electrophoresis*, *21*(1), 27–40. https://doi.org/10.1002/(SICI)1522-2683(20000101)21:1<27::AID-ELPS27>3.0.CO;2-C [pii] 10.1002/(SICI)1522-2683(20000101)21:1<27::AID-ELPS27>3.0.CO;2-C

Yan, Q., Dong, H., Su, J., Han, J., Song, B., Wei, Q., & Shi, Y. (2018). A Review of 3D Printing Technology for Medical Applications. *Engineering*, *4*(5), 729–742. https://doi.org/10.1016/j.eng.2018.07.021

Yu, H. S., Scalera, J., Khalid, M., Touret, A. S., Bloch, N., Li, B., … Anderson, S. W. (2017). Texture analysis as a radiomic marker for differentiating renal tumors. *Abdominal Radiology*, *42*(10), 2470–2478. https://doi.org/10.1007/s00261-017-1144-1

Yuheng, S., & Hao, Y. (2017). Image Segmentation Algorithms Overview, *1*. Retrieved from http://arxiv.org/abs/1707.02051

Zakaly, H. M., Abouhaswa, A. S., Issa, S. A. M., Mostafa, M. Y. A., Pyshkina, M., & El-Mallawany, R. (2020). Optical and nuclear radiation shielding properties of zinc borate glasses doped with lanthanum oxide. *Journal of Non-Crystalline Solids*, *543*(May), 120151. https://doi.org/10.1016/j.jnoncrysol.2020.120151

Zhou, L., Zhang, Z., Chen, Y. C., Zhao, Z. Y., Yin, X. D., & Jiang, H. B. (2019). A Deep Learning-Based Radiomics Model for Differentiating Benign and Malignant Renal Tumors. *Translational Oncology*, *12*(2), 292–300. https://doi.org/10.1016/j.tranon.2018.10.012

Zulkifli Ahmad. (2012). *Polymer Dielectric Materials, Dielectric Material*. (Marius Alexandru Silaghi, Ed.), *iIntechOpen*. https://doi.org/10.5772/50638